Peritoneal Effluent MicroRNA Profile in Encapsulating Peritoneal Sclerosis

Kun-Lin Wu
Taoyuan Armed Forces General Hospital
Che-Yi Chou
Asia University Hospital
An-Lun Li
National Central University
Chien-Lung Chen
Landseed International Hospital
Jen-chieh Tsai
National Tsing Hua University
I-Kuan Wang
China Medical University Hospital
Chiung-Tong Chen
National Health Research Institutes
Chin-Chung Tseng
National Cheng Kung University Hospital
Jin-Bor Chen
Kaohsiung Chang Gung Memorial Hospital
Yi-Fan Chan
National Central University
Hui-Yin Chang
National Central University
Chiu-Ching Huang
China Medical University Hospital
Nianhan Ma (nianhan.ma@gmail.com)
National Central University

Research Article

Keywords: peritoneal dialysis, encapsulating peritoneal sclerosis, microRNA, biomarker

Posted Date: October 1st, 2021

DOI: https://doi.org/10.21203/rs.3.rs-832435/v2

Abstract

Encapsulating peritoneal sclerosis (EPS) is a catastrophic complication of chronic peritoneal dialysis (PD). Late diagnosis is associated with high mortality. With the advancement of new diagnostic technologies, such as microRNA (miRNA), we attempted to develop a noninvasive test to assist in the diagnosis of EPS. The eight-hour PD effluents were collected from 71 non-EPS and 56 EPS patients. The screening set included 28 samples (20 of non-EPS vs. 8 of EPS). After analyzing the ratio values of two miRNA expression levels from the high-throughput real-time PCR-array of 377 miRNAs, eight candidate miRNAs were selected. The prediction model was conducted using 127 samples (71 of non-EPS vs 56 of EPS) to produce an area under the curve (AUC) value of the miRNA classifier. Candidate miRNAs were also verified by single real-time PCR. The ratios of the five miRNAs with the top five ROC values were selected to calculate the combined AUC by multiple logistic regression. The AUC value to detect EPS with the five miRNA ratios was 0.8929 with an accuracy of 78.7%. The accuracy of the EPS diagnosis was further optimized to 94.1% after considering clinical characteristics (AUC value 0.9931). A signature-based model of clinical characteristics and miRNA expression in PD effluents can efficiently assist in the diagnosis of EPS, thus preventing the catastrophic prognosis.

Introduction

The mortality rate in chronic kidney disease (CKD) has increased since 1990. In 2017, there were 697.5 million patients, there was an estimated prevalence of 9.1% in the world's population, and 1.2 million people died [1]. In patients with a progression of CKD to end-stage renal disease (ESRD), renal replacement therapy is a lifesaving treatment through hemodialysis, peritoneal dialysis (PD), or renal transplantation. Approximately 78% of people with end-stage renal disease receive dialysis, of which 89% and 11% are treated by hemodialysis and peritoneal dialysis, respectively [2,3]. The number and prevalence of patients treated with peritoneal dialysis are estimated to be increasing globally due to certain factors, including the simplicity of the technique, and the low requirements for machinery and electricity [2,4,5].

Encapsulating peritoneal sclerosis (EPS) is a fatal complication in patients on peritoneal dialysis for end-stage renal disease. The prevalence of EPS has been reported to be 0.4%- 8.9%, and its incidence rate is 0.7–13.6 per 1,000 patient-years [6–8]. Although drugs, such as corticosteroids [7,9], tamoxifen [10,11], and immunosuppressive agents, have been reported to improve the outcome of EPS, the mortality rate for EPS remains high (25–55%), with death within one year following the diagnosis [8]. It has been reported that the risk of occurrence significantly rises with a longer duration of PD [6]. The risk factors for EPS include a higher dialysate glucose exposure, the duration of peritoneal dialysis, younger age at the start of PD, frequency of peritonitis, change in peritoneal membrane characteristics with fast transporter and ultrafiltration failure, abdominal surgery, ß-blocker use, and kidney transplantation [6–8, 10,12,13]. EPS formation has been proposed in which the bowel entrapped by inflammatory and fibrotic capsules of the peritoneum leads to a bowel obstruction [14,15]. The diagnosis of EPS is complicated and is mainly based on a combination of functional and structural characteristics [6,12]. A number of manifestations can cause

the progression of EPS from early symptoms (bloody ascites, nausea, and change of defecation) to severe symptoms (severe abdominal pain, vomiting, anorexia, malnutrition, weight loss, and the development of an abdominal mass which would indicate various severities of bowel obstruction). Imaging studies are used to confirm the structural changes of EPS. Thickened peritoneum, peritoneal calcification, bowel tethering, fluid loculation, and bowel dilatation in computed tomographic scans indicate the structural changes found in EPS [6,12,15]. Imaging studies are the most common diagnostic tools to confirm the clinical diagnosis of EPS. Thickening of the peritoneum develops in many patients with long-term PD. However, diagnostic imaging has its limitation in detecting the early stage of EPS (pre-EPS or the inflammatory stage) due to uncertain structure changes [6,12,15]. The current criteria for diagnosing EPS, including the clinical manifestations of bowel obstruction and peritoneal sclerosis confirmed by macroscopic or radiological findings, are not specific, and thus delays the diagnosis.

Biomarkers from peritoneal effluent can be acquired easily and are potentially useful to improve the prediction of early EPS. It has been reported that the combination of an effluent rate having low CA125 (< 33 U/min) and high IL-6 (> 350 pg/min) had a sensitivity of 70% and a specificity of 89% for EPS diagnosis [16]. In addition, effluent plasminogen activator inhibitor 1 (PAI-1) is upregulated in EPS and is linked to progressive peritoneal sclerosis with a time-specific receiver operating characteristic (ROC) curve of 0.71–0.77 [17]. It is unlikely that a single biomarker is sufficient for EPS detection and the clinical values of the above biomarker candidates require careful validation.

MicroRNAs (miRNAs) are posttranscriptional regulators of gene expression, and they modulate a broad range of physiological functions [18]. In biological fluids, circulating miRNAs in exosomes are packaged to maintain their stability and prevent their degradation [19]. Moreover, previous studies have reported that miRNA expression levels in the peritoneal fluid are associated with changes in peritoneal transport characteristics and fibrosis [20,21]. Therefore, circulating miRNAs in PD effluent could serve as potential biomarkers for the diagnosis and monitoring of EPS. We designed this study to investigate the use of the expression of several miRNAs as noninvasive and highly sensitive molecular biomarkers of EPS.

Methods And Materials

Study Design and Participants

The study protocol was approved by the medical ethics committee of three medical centers in Taiwan (the China Medical University Hospital, CMUH103-REC2-070; the National Chen Kung University Hospital, B-ER-104-069; and the Kaohsiung Chang Gung Memorial Hospital, 100-2661B) [23]. The study was conducted in accordance with the Declaration of Helsinki, and the institutional ethical review board approved the protocol. Informed consent was obtained from all subjects. A total of 127 samples (56 EPS and 71 non-EPS) from PD patients participated in this study. All PD patients satisfied the following eligibility criteria: peritoneal dialysis for more than 3 months, age > 20 years old, and EPS or non-EPS diagnosis. The diagnostic criteria of EPS were based on clinical symptoms of intermittent subacute bowel obstruction (bloody ascites, appetite loss, nausea, diarrhea, abdominal pain, constipation, and

mass-like lesion of abdomen) and structural features by computed tomography (thickened peritoneum, peritoneal calcification, bowel thickening, bowel tethering, and bowel dilatation) [6,34]. All the patients were identified by 2 experienced nephrologists and a radiologist, and anonymous, but age, sex, medical history, laboratory data, and peritoneal equipment test measurements were collected for further analysis. The samples were collected from PD effluent that was drained out from the peritoneal cavity after 8 hours of dialysis. The effluent was centrifuged to remove cells and was stored at −80 °C until processing.

RNA extraction

Total RNA was extracted from one milliliter of PD effluent by using TRIzol® LS Reagent (10296010, Thermo Fisher Scientific) and the mirVana™ miRNA Isolation Kit (AM1560, Thermo Fisher Scientific) according to the standard protocol. The spiked-in control of *Caenorhabditis elegans* miR-39-3p (5'-UCACCGGGUGUAAAUCAGC UUG-3') for technical alterability was performed as previously described [35,36]. We added 20 μl of 95 °C RNase-free water to the column and incubated it for 1 min before centrifugation at 13,000 × g for 3 min at 4 °C to elute total RNA. Then, it was stored at −80 °C.

High-throughput and single real-time quantitative reverse transcriptase polymerase chain reaction analysis.

The megaplex RT primers of human pool A were used to simultaneously synthesize cDNAs (4399966, Thermo Fisher Scientific). In total, 377 miRNA assays were included in the miRNA array card A (4398965, Thermo Fisher Scientific). The expression levels of candidate miRNAs were further determined by a single miRNA assay according to the standard protocol (4427975, Thermo Fisher Scientific). TaqMan 2x Universal PCR master mix without UNG was used for PCR (23053541, Roche). The Abi Vii7 qRT-PCR system with the heat block of plate adaptor or 384-well plates was used for the high-throughput array cards or the miRNA single assays, respectively.

Statistical analysis

Clinical characteristics between non-EPS and EPS patients were evaluated using the Student's t-test and Pearson's chi-squared test for each variable using SPSS. High-throughput data from TaqMan array cards were analyzed by using ViiA7 software. The expression level of PD effluent circulating miRNA was calculated by the $2^{-\Delta CT}$ method. We used the Student's t-test to evaluate the difference in miRNA expression levels. All tests were two-tailed and were assessed by Levene's test. Multiple logistic regression was performed by Sigma plot software to combine different candidate miRNAs. The receiver operating characteristic (ROC) curve was generated by GraphPad Prism 6 software to calculate the sensitivity, specificity, and area under the curve (AUC) to determine the diagnostic efficiency.

Results

Identification of differentially expressed PD effluent miRNAs between EPS and non-EPS in PD patients.

We aimed to develop a noninvasive diagnostic tool for EPS detection in PD patients. In total, 127 PD patients were enrolled in the study (Fig. 1). In the screening set, miRNA expression levels of PD effluent were profiled quantitatively by high-throughput real-time PCR arrays, which included 377 miRNA assays from 28 PD effluent samples (8 EPS and 20 non-PES). There is no suitable internal control of miRNA or noncoding RNA to normalize miRNA expression levels in PD effluent. The ratio of two miRNA expression levels from the same sample can be calculated to eliminate the normalization issue of extracellular miRNA expression. The values of the ratio of two miRNA expression levels between the EPS and non-EPS samples were analyzed by the fold change and the Student's t-test (Fig. 2). Five ratios of miRNAs (miR-483-5p/miR-597, miR-422a/miR-518e, miR-202-3p/miR-597, miR-155-5p/miR-17-5p, and miR-597/miR-100-5p) were present with a high statistical significance and fold change between the EPS and non-EPS groups (Fig. 2). Furthermore, eight candidate miRNAs among the five ratios of miRNAs (miR-17-5p, miR-100-5p, miR-155-5p, miR-202-3p, miR-422a, miR-483-5p, miR-518e, and miR-597) were selected for further verification and the establishment of the prediction model.

We examined the expression of eight candidate miRNAs from the screening set by single qRT-PCR in the validation set, which included 127 PD effluent samples (56 EPS and 71 non-EPS). The expression levels of seven miRNAs among eight candidate miRNAs were significantly decreased in the EPS group (p value: miR-17-5p: 0.0049, miR-100-5p: 6.1E-09, miR-155-5p: 2.4E-10, miR-202-3p: 2.5E-06, miR-422a: 7.6E-09, miR-483-5p: 0.00066 and, miR-597: 0.0009) (Fig. 3). The area under the receiver operating characteristic curve (AUC) is the most commonly used performance measure to indicate the discriminative ability. To develop a miRNA signature-based model for assessing the risk of EPS, we carried out a ROC analysis. All miRNA combination ratios were calculated by randomly selecting two miRNAs expressed among seven candidate miRNAs in the PD effluent. We selected the top five AUC values: miR-422a/miR-17-5p, miR-202-3p/miR-483-5p, miR-422a/miR-483-5p, miR-202-3p/miR-155-5p, and miR-202-3p/miR-17-5p, with AUC values of 0.7115, 0.7438, 0.7310, 0.6962, and 0.707, respectively (Fig. 4). Furthermore, these five ratios of miRNAs contained only five miRNAs, and the expression levels of these top five miRNAs were also significantly decreased in the EPS group (Fig. 5).

The development of prediction model to identify EPS in PD patients

Next, we utilized multiple logistic regression calculation formulas by combining five ratios of miRNA expression levels to establish a proper model to estimate the EPS in PD patients. The predicted probability of EPS was calculated by: Logit P = -3.215 + (1.499 * miR-422a/miR-17-5p) + (1.415 *miR-202-3p/miR-483-5p) + (1.428 * miR-422a/miR-483-5p) + (1.521 * miR-202-3p/miR-155-5p) + (0.349 * miR-202-3p/miR-17-5p). As a result, the AUC value of the combined five ratios of miRNAs expressions from 127 effluents increased to 0.8929 with a sensitivity of 91.1% and a specificity of 69% with a cutoff value of >-0.8585 (95% CI = 0.8364 to 0.9476), compared with the use of each ratio of miRNAs alone (Fig. 6A). The signature score of the combined five ratios of miRNA expressions in EPS is significantly higher than that in non-EPS of PD patients (Fig. 6B).

Moreover, seven PD patients developed EPS during the interval of 0.5-4 years in our study, and their signature scores from non-EPS and EPS effluents were compared (Fig. 6C). Despite uncertain symptoms, our prediction model accurately predict thirteen results from fourteen samples. Nausea, vomiting and abdominal pain developed in patient 1. Esophagogastroduodenoscopy revealed duodenal ulcers with duodenitis and a partial gastric outlet obstruction when the measured score was − 3.215. Her symptoms improved after omeprazole therapy. Severe abdominal pain with rebounding pain developed one year later, and free air, bowel tethering, fluid loculation, and local bowel dilatation were confirmed by computed tomography. The intraoperative findings were that there was gangrene of the intestines, which was encapsulated by a leathery peritoneum and a dirty ascites. Patient 2 developed bacterial peritonitis in *Pseudomonas aeruginosa* infection, and the patient developed abdominal distension and intermittent pain. The diagnosis of EPS was suspected from our measured score and then was confirmed after noting a thickened peritoneum on abdominal computed tomography. Although the signature score in patient 3 without EPS was incorrect, the trend of the signature scores from low to high was noticed. The change in signature scores may indicate the development of EPS.

The optimization of EPS prediction model with the clinical characteristics of patients

As shown in Table 1, there were 85 PD patients (34 EPS and 51 non-EPS) with clinical data. EPS patients tended to sustain more episodes of peritonitis ($p < 0.001$) as well as a longer PD duration ($p = 0.004$). Moreover, C-reactive protein (CRP) levels were significantly higher ($p = 0.027$) in the EPS group, which may implicate the potential inflammation of EPS by high glucose dialysate and presence of infection. The etiology of ESRD and comorbidities were similar between PD patients with EPS and non-EPS patients. Similar results showed an increased incidence of EPS with a longer duration of PD and active inflammation with a higher CRP value [16,22,23]. The predictive value of the clinical characteristics with PD duration (cutoff value: > 10.5 years) and CRP levels (cutoff value: > 2.24 mg/dl) was estimated to detect EPS, and the AUC was 0.848 (Fig. 7A and 7B). ROC analysis with the five miRNA ratios was shown to distinguish non-EPS and EPS of PD patients with an AUC of 0.9426. For optimization, we combined the values of the five ratios of miRNAs with information on the duration of PD and the CRP value, which was calculated by: Logit P = -8.014 + (3.960 * PD duration) + (1.388 * CRP) + (1.989 * miR-422a/miR-17-5p) + (2.710 * miR-202-3p/miR-483-5p) + (2.081 * miR-422a/miR-483-5p) + (2.354 * miR-202-3p/miR-155-5p) + (0.357 * miR-202-3p/miR-17-5p). The accuracy of the detection of EPS was further improved, with an AUC of 0.9931, a sensitivity of 100% and a specificity of 94.1% (95% CI = 0.9819 to 1) (Fig. 7).

Table 1
Clinical characteristics of EPS and control patients

Factor	Non-EPS	EPS	P value
n	51	34	
Male: Female	16:35	13:21	0.51
Age (year)	58 ± 11.3	52.8 ± 14.2	0.06
Weight (kg)	54.4 ± 8.3	51.9 ± 10.5	0.24
Height (cm)	156.6 ± 6.7	156.3 ± 10.37	0.87
PD duration (year)	9.4 ± 3.5	12.8 ± 5	0.004
Peritonitis (episodes)	0.10 ± 0.30	0.45 ± 0.56	< 0.001
PET			
D/P creatinine			< 0.001
H	17.6%	66.7%	
HA	52.9%	16.7%	
LA	29.4%	13.3%	
L	0%	3.3%	
D/P glucose			< 0.001
H	9.8%	33.3%	
HA	51%	33.3%	
LA	39.2%	16.7%	
L	0%	16.7%	
Hemoglobin (g/dl)	10.2 ± 1.4	10.1 ± 2.0	0.79
Albumin (g/dl)	3.6 ± 0.3	3.5 ± 0.5	0.96
Calcium (mg/dl)	9.7 ± 0.9	9.4 ± 0.8	0.12
Phosphorus (mg/dl)	5.2 ± 1.2	4.6 ± 1.2	0.066
CRP (mg/dl)	0.7 ± 0.8	25.2 ± 10.8	0.027
iPTH (pg/ml)	517.3 ± 478.9	684.9 ± 710.6	0.2

EPS: encapsulated peritoneal sclerosis, PD: peritoneal dialysis, PET: peritoneal equilibration test, D/P: The ratio of solute concentrations in dialysate and plasma, CRP: C-reactive protein, iPTH: intact PTH, H, HA, LA, and L: high, high average, low average and low level of peritoneal transport status.

High transport of peritoneal equilibration test with fast waste removal and limited ultrafiltration was found in EPS patients because of the pathologic changes in the peritoneum, such as angiogenesis and fibrosis (Table 1). Our score distribution was significantly positively correlated with the transport rate of creatinine, indicating these scores were linked to the functional impairment of peritoneal membrane. (Fig. 8).

Discussion

PD patients are currently diagnosed with EPS based on functional and structural features, but nonspecific and uncertain symptoms lead to a delay in diagnosis [12,14]. We investigated the expression of miRNAs from the effluent of PD patients to establish a prediction model to identify EPS. An EPS prediction model was established by combined five ratios of miRNA expression: miR-202-3p/miR-17-5p, miR-202-3p/miR-155-5p, miR-202-3p/miR-485-5p, miR-422a/miR-17-5p, and miR-422a/miR-485-5p (Fig. 6). After consideration of the clinical characteristics, PD duration, and CRP level, the accuracy of the EPS prediction model was further optimized (Fig. 7).

The pathophysiology of EPS is described as a multiple-hit process in which mesothelial-mesenchymal transition (MMT) plays a central role [12,14,24]. It has been reported that fibroblasts derived from mesothelial cells can participate in inflammatory responses, extracellular matrix accumulation, and angiogenesis [24]. The biomolecules involved in MMT have the potential to assess and monitor the pathophysiological processes. miRNAs are ubiquitous and functional modulators in body fluids. Specific miRNAs with concentrations in body fluids can be used as potential biomarkers for detecting and monitoring various pathophysiological conditions [18,19]. Our study reveals that the expression of five miRNAs in the prediction model, miR-17-5p, miR-155-5p, miR-202-3p, miR-422a, and miR-483-5p, was decreased in the EPS patients compared with the non-EPS patients (Fig. 4). MiR-17-5p has been reported to regulate peritoneal fibrosis through the positive feedback loop of HIF1A and VEGF [25]. MiR-155-5p has been implicated as a multifunctional molecule that includes SHIP1, HBP1, SOCS1, BCL6, CARHSP1, and MAP3K10, which are linked to atherosclerotic inflammatory processes and are regulated in coronary artery disease [26]. Moreover, miR-155-5p was induced by VEGF to target the E2F2 transcription factor to promote angiogenesis [27]. In scleroderma fibrosis, overexpression of miR-202-3p induced collagen disposition by targeting MMP1 [28]. Overexpression of miRNA-202-3p targeted TRPM6 to alleviate the myocardial ischemia-reperfusion injury induced by the TGF-β1/Smad signaling pathway [29]. MiR-422a directly targeted KLK4 mRNA to modulate the renal kallikrein-kinin system with pleiotropic functions in inflammation, coagulation, angiogenesis, and vascular physiology [30,31]. Overexpression of miR-483-5p inhibited angiogenesis by targeting serum response factor [32]. Interestingly, the literature showed that these five miRNAs identified in our study are associated with the MMT process. Therefore, these miRNAs may play differential key roles in the pathophysiological process of EPS. Further advanced studies will be designed to investigate their functions in EPS.

The factors involved in inflammation, angiogenesis, and fibrosis of MMT may have the potential to be diagnostic biomarkers for EPS [12,16,17,33]. The combination of low CA125 and high IL-6 for the diagnosis of EPS has also been reported to associate with decreased mesothelial cell mass and inflammation, respectively [16]. In addition, effluent plasminogen activator inhibitor 1 was upregulated by transforming growth factor ß1 and leads to progressive peritoneal sclerosis [17]. Moreover, a recent study showed that both the level of matrix metalloproteinase-2 in effluent and the PD duration can improve the estimation of the risk of EPS [33]. A longer duration of PD and active inflammation with a higher CRP value has been implicated for an increased risk of EPS [16,22,23]. However, the sample size of EPS was less than twenty, which is low sample size for confirmation to be a reliable biomarker, and the sensitivity was also low in a previous study. In this study, we developed a miRNA signature-based model to differentiate 56 EPS from 71 non-EPS patients, and the AUC was 0.8929. The combination of the five ratios of miRNAs and the duration of PD and the CRP levels increased the accuracy of the EPS detection, with an AUC of 0.9931. The results indicated that the prediction model using the miRNA expressions with clinical characteristics can be a potential tool to detect EPS in chronic PD patients.

Some limitations of our study are present. First, the number of EPS patients was limited, which may lead to potential bias. Second, the clinical data in some patients were lost because we collected PD samples with anonymous information from several hospitals. Third, the functions of the five identified miRNAs were not investigated in the development of peritoneal sclerosis.

In PD patients, EPS is a catastrophic disease with a cocoon of the bowel that is induced by long-term exposure to high glucose PD fluid, drugs, infection, and systemic inflammatory diseases. Diagnosis is often delayed when the disorder is combined with nonspecific clinical characteristics. In our study, a signature-based model of the combined clinical characteristics and the five ratios of five miRNA expression levels could efficiently monitor and detect EPS.

Declarations

Acknowledgements

This work was supported by the following programs: Academia Sinica, Taiwan (BM103010089 and BM104010113 to CC Huang), the Taiwan Department of Health Cancer Research Center of Excellence (DOH101-TD-C-111-005), Ministry of Science and Technology, Taiwan (MOST 109-2628-B-008-001 and MOST 110-2823-8-008-002), the National Central University-Landseed Hospital United Research Center (NCU-LSH-109-A-004), and Taoyuan Armed Forces General Hospital (TYAFGH-D-109024).

Authors' contributions

All authors read and approved the final manuscript. K.L.W., A.L.L., and J.C.T. performed the experiments; K.L.W., C.Y.C., A.L.L, J.C.T., C.C.H., and N.H.M. contributed to designing research and discussing findings; K.L.W., C.Y.C, A.L.L., C.L.C., J.C.T., I.K.W., Y.F.C., and H.Y.C. analyzed data; K.L.W.,

C.Y.C., C.C.H. and N.H.M. wrote the manuscript; C.L.C., I.K.W., C.C.T., and J.B.C. sample collection; C.T.C., C.C.T., J.B.C., C.C.H., and N.H.M. supervised the work.

Additional Information

All authors declare no competing interests.

Data availability

The datasets analysed during the current study are available from the corresponding author on reasonable request.

References

1. Collaboration, G. B. D. C. K. D. Global, regional, and national burden of chronic kidney disease, 1990–2017: a systematic analysis for the Global Burden of Disease Study 2017., **395**, 709–733 https://doi.org/10.1016/S0140-6736(20)30045-3 (2020).
2. Li, P. K. *et al.* Changes in the worldwide epidemiology of peritoneal dialysis. *Nat Rev Nephrol*, **13**, 90–103 https://doi.org/10.1038/nrneph.2016.181 (2017).
3. Liyanage, T. *et al.* Worldwide access to treatment for end-stage kidney disease: a systematic review., **385**, 1975–1982 https://doi.org/10.1016/S0140-6736(14)61601-9 (2015).
4. Finkelstein, F. O. *et al.* Peritoneal dialysis in the developing world: recommendations from a symposium at the ISPD meeting 2008. Perit Dial Int 29, 618–622(2009).
5. Jain, A. K., Blake, P., Cordy, P. & Garg, A. X. Global trends in rates of peritoneal dialysis. *J Am Soc Nephrol*, **23**, 533–544 https://doi.org/10.1681/ASN.2011060607 (2012).
6. Brown, E. A. *et al.* Length of Time on Peritoneal Dialysis and Encapsulating Peritoneal Sclerosis - Position Paper for ISPD: 2017 Update. *Perit Dial Int*, **37**, 362–374 https://doi.org/10.3747/pdi.2017.00018 (2017).
7. Kawanishi, H. *et al.* Encapsulating peritoneal sclerosis in Japan: a prospective, controlled, multicenter study. *Am J Kidney Dis*, **44**, 729–737 (2004).
8. Brown, M. C., Simpson, K., Kerssens, J. J. & Mactier, R. A. & Scottish Renal, R. Encapsulating peritoneal sclerosis in the new millennium: a national cohort study. *Clin J Am Soc Nephrol*, **4**, 1222–1229 https://doi.org/10.2215/CJN.01260209 (2009).
9. Kuriyama, S. & Tomonari, H. Corticosteroid therapy in encapsulating peritoneal sclerosis. *Nephrol Dial Transplant*, **16**, 1304–1305 https://doi.org/10.1093/ndt/16.6.1304 (2001).
10. Korte, M. R. *et al.* Tamoxifen is associated with lower mortality of encapsulating peritoneal sclerosis: results of the Dutch Multicentre EPS Study. *Nephrol Dial Transplant*, **26**, 691–697 https://doi.org/10.1093/ndt/gfq362 (2011).
11. Summers, A. M. *et al.* Single-center experience of encapsulating peritoneal sclerosis in patients on peritoneal dialysis for end-stage renal failure. *Kidney Int*, **68**, 2381–2388

https://doi.org/10.1111/j.1523-1755.2005.00701.x (2005).

12. Korte, M. R., Sampimon, D. E., Betjes, M. G. & Krediet, R. T. Encapsulating peritoneal sclerosis: the state of affairs. *Nat Rev Nephrol*, **7**, 528–538 https://doi.org/10.1038/nrneph.2011.93 (2011).
13. Korte, M. R., Habib, S. M., Lingsma, H., Weimar, W. & Betjes, M. G. Posttransplantation encapsulating peritoneal sclerosis contributes significantly to mortality after kidney transplantation. *Am J Transplant*, **11**, 599–605 https://doi.org/10.1111/j.1600-6143.2010.03434.x (2011).
14. Augustine, T., Brown, P. W., Davies, S. D., Summers, A. M. & Wilkie, M. E. Encapsulating peritoneal sclerosis: clinical significance and implications. *Nephron Clin Pract*, **111**, c149–154 discussion c154https://doi.org/10.1159/000191214 (2009).
15. Singhal, M. *et al.* Encapsulating Peritoneal Sclerosis: The Abdominal Cocoon., **39**, 62–77 https://doi.org/10.1148/rg.2019180108 (2019).
16. Sampimon, D. E. *et al.* Early diagnostic markers for encapsulating peritoneal sclerosis: a case-control study. *Perit Dial Int*, **30**, 163–169 https://doi.org/10.3747/pdi.2009.00022 (2010).
17. Lopes Barreto, D., Struijk, D. G. & Krediet, R. T. Peritoneal effluent MMP-2 and PAI-1 in encapsulating peritoneal sclerosis. *Am J Kidney Dis*, **65**, 748–753 https://doi.org/10.1053/j.ajkd.2014.10.022 (2015).
18. Gebert, L. F. R. & MacRae, I. J. Regulation of microRNA function in animals. *Nat Rev Mol Cell Biol*, **20**, 21–37 https://doi.org/10.1038/s41580-018-0045-7 (2019).
19. Weber, J. A. *et al.* The microRNA spectrum in 12 body fluids. *Clin Chem*, **56**, 1733–1741 https://doi.org/10.1373/clinchem.2010.147405 (2010).
20. Che, M. *et al.* The MicroRNA-199a/214 Cluster Targets E-Cadherin and Claudin-2 and Promotes High Glucose-Induced Peritoneal Fibrosis. *J Am Soc Nephrol*, **28**, 2459–2471 https://doi.org/10.1681/ASN.2016060663 (2017).
21. Szeto, C. C. *et al.* Peritoneal dialysis effluent miR-21 and miR-589 levels correlate with longitudinal change in peritoneal transport characteristics. *Clin Chim Acta*, **464**, 106–112 https://doi.org/10.1016/j.cca.2016.11.020 (2017).
22. Habib, S. M., Korte, M. R. & Betjes, M. G. Lower mortality and inflammation from post-transplantation encapsulating peritoneal sclerosis compared to the classical form. *Am J Nephrol*, **37**, 223–230 https://doi.org/10.1159/000348267 (2013).
23. Tseng, C. C. *et al.* Incidence and outcomes of encapsulating peritoneal sclerosis (EPS) and factors associated with severe EPS. *PLoS One*, **13**, e0190079 https://doi.org/10.1371/journal.pone.0190079 (2018).
24. Aroeira, L. S. *et al.* Epithelial to mesenchymal transition and peritoneal membrane failure in peritoneal dialysis patients: pathologic significance and potential therapeutic interventions. *J Am Soc Nephrol*, **18**, 2004–2013 https://doi.org/10.1681/ASN.2006111292 (2007).
25. Li, J. *et al.* HIF1A and VEGF regulate each other by competing endogenous RNA mechanism and involve in the pathogenesis of peritoneal fibrosis. *Pathol Res Pract*, **215**, 644–652 https://doi.org/10.1016/j.prp.2018.12.022 (2019).

26. Cao, R. Y. *et al.* The Emerging Role of MicroRNA-155 in Cardiovascular Diseases. *Biomed Res Int* 2016, 9869208, doi:10.1155/2016/9869208 (2016).
27. Yang, D., Wang, J., Xiao, M., Zhou, T. & Shi, X. Role of Mir-155 in Controlling HIF-1alpha Level and Promoting Endothelial Cell Maturation. *Sci Rep*, **6**, 35316 https://doi.org/10.1038/srep35316 (2016).
28. Zhou, B. *et al.* MicroRNA-202-3p regulates scleroderma fibrosis by targeting matrix metalloproteinase 1. *Biomed Pharmacother*, **87**, 412–418 https://doi.org/10.1016/j.biopha.2016.12.080 (2017).
29. Wu, H. Y., Wu, J. L. & Ni, Z. L. Overexpression of microRNA-202-3p protects against myocardial ischemia-reperfusion injury through activation of TGF-beta1/Smads signaling pathway by targeting TRPM6., **18**, 621–637 https://doi.org/10.1080/15384101.2019.1580494 (2019).
30. Serino, G., Curci, C. & Schena, F. P. Role of miR-422a and kallikrein-related peptidase 4 implicated in the development of lupus nephritis. Do we work in this direction? *Nephrol Dial Transplant*, **31**, 683–685 https://doi.org/10.1093/ndt/gfv396 (2016).
31. Krasoudaki, E. *et al.* Micro-RNA analysis of renal biopsies in human lupus nephritis demonstrates up-regulated miR-422a driving reduction of kallikrein-related peptidase 4. *Nephrol Dial Transplant*, **31**, 1676–1686 https://doi.org/10.1093/ndt/gfv374 (2016).
32. Qiao, Y. *et al.* MiR-483-5p controls angiogenesis in vitro and targets serum response factor. *FEBS Lett*, **585**, 3095–3100 https://doi.org/10.1016/j.febslet.2011.08.039 (2011).
33. Chou, C. Y., Tseng, C. C., Chen, J. B., Hung, C. C. & Huang, C. C. A Matrix Metalloproteinase-2-Based Nomogram to Assess the Risk of Encapsulating Peritoneal Sclerosis in Peritoneal Dialysis Patients. Biomed Res Int 2021, 6666441, doi:10.1155/2021/6666441 (2021).
34. Tarzi, R. M. *et al.* Assessing the validity of an abdominal CT scoring system in the diagnosis of encapsulating peritoneal sclerosis. *Clin J Am Soc Nephrol*, **3**, 1702–1710 https://doi.org/10.2215/CJN.01820408 (2008).
35. Chen, C. L. *et al.* Plasma miRNA profile is a biomarker associated with urothelial carcinoma in chronic hemodialysis patients. *Am J Physiol Renal Physiol*, **316**, F1094–F1102 https://doi.org/10.1152/ajprenal.00014.2019 (2019).
36. Li, A. L. *et al.* microRNA expression pattern as an ancillary prognostic signature for radiotherapy. *J Transl Med*, **16**, 341 https://doi.org/10.1186/s12967-018-1711-4 (2018).

Figures

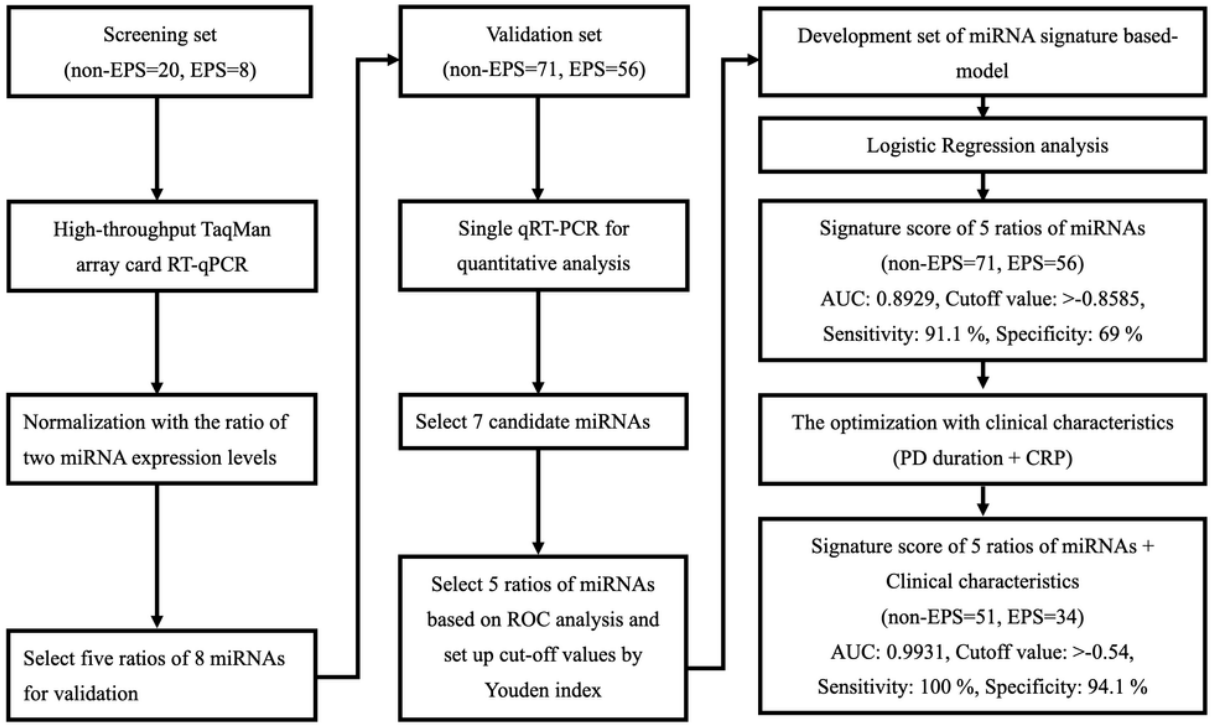

Figure 1

The flowchart of this study.

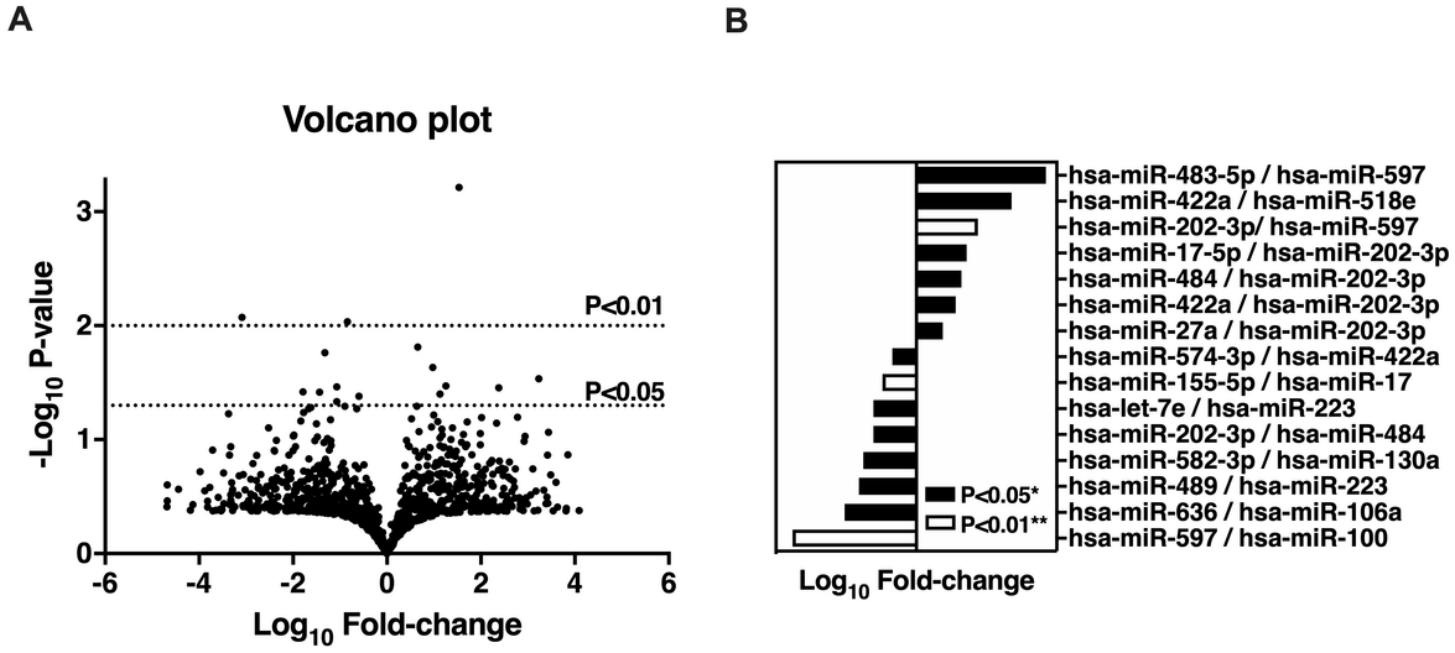

Figure 2

The selection of candidate miRNAs from effluents of EPS and non-EPS patients. MiRNA expression levels of PD effluent were profiled quantitatively by high-throughput real-time PCR arrays, which included 377 miRNA assays from 28 PD effluent samples (8 EPS and 20 non-PES). The volcano plot shows the distribution of miRNA ratios by the fold change and P value. There were 3 ratios with a P value < 0.01 and 12 ratios with a P value < 0.05 (A). In the bar chart, three ratios with a P value < 0.01 were selected. Two ratios with higher fold changes (P value < 0.05) were also selected (B).

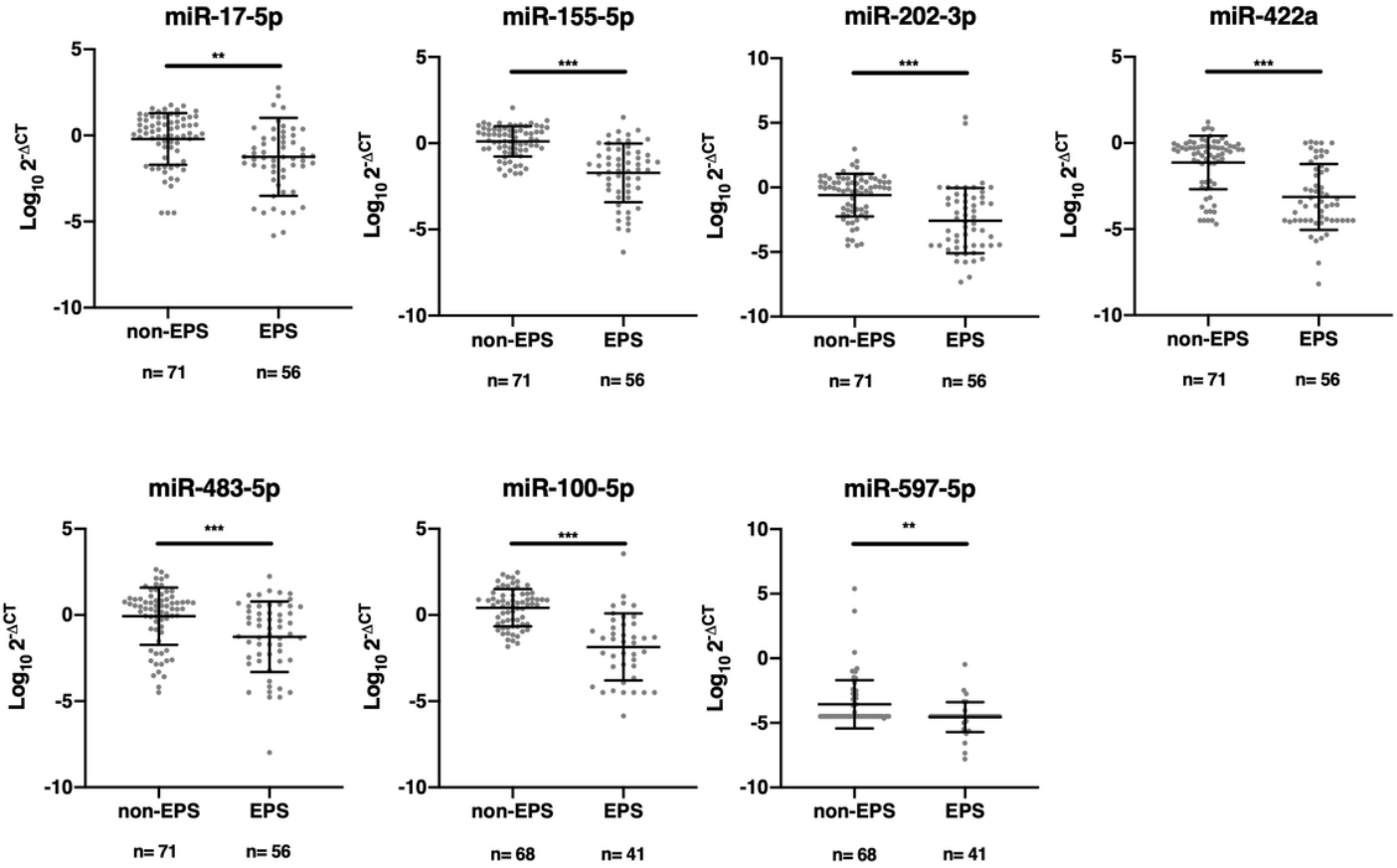

Figure 3

Scatter plots of single miRNA expression levels between the EPS and non-EPS groups. Significant changes in the miRNA expression levels in the effluent of PD patients by qRT-PCR using RNU6 as a control. The Y axis presents the expression level (Log10 2-ΔCT). The p-value was analyzed by the Student's t-test for each miRNA. **P value < 0.01; ***P value < 0.001

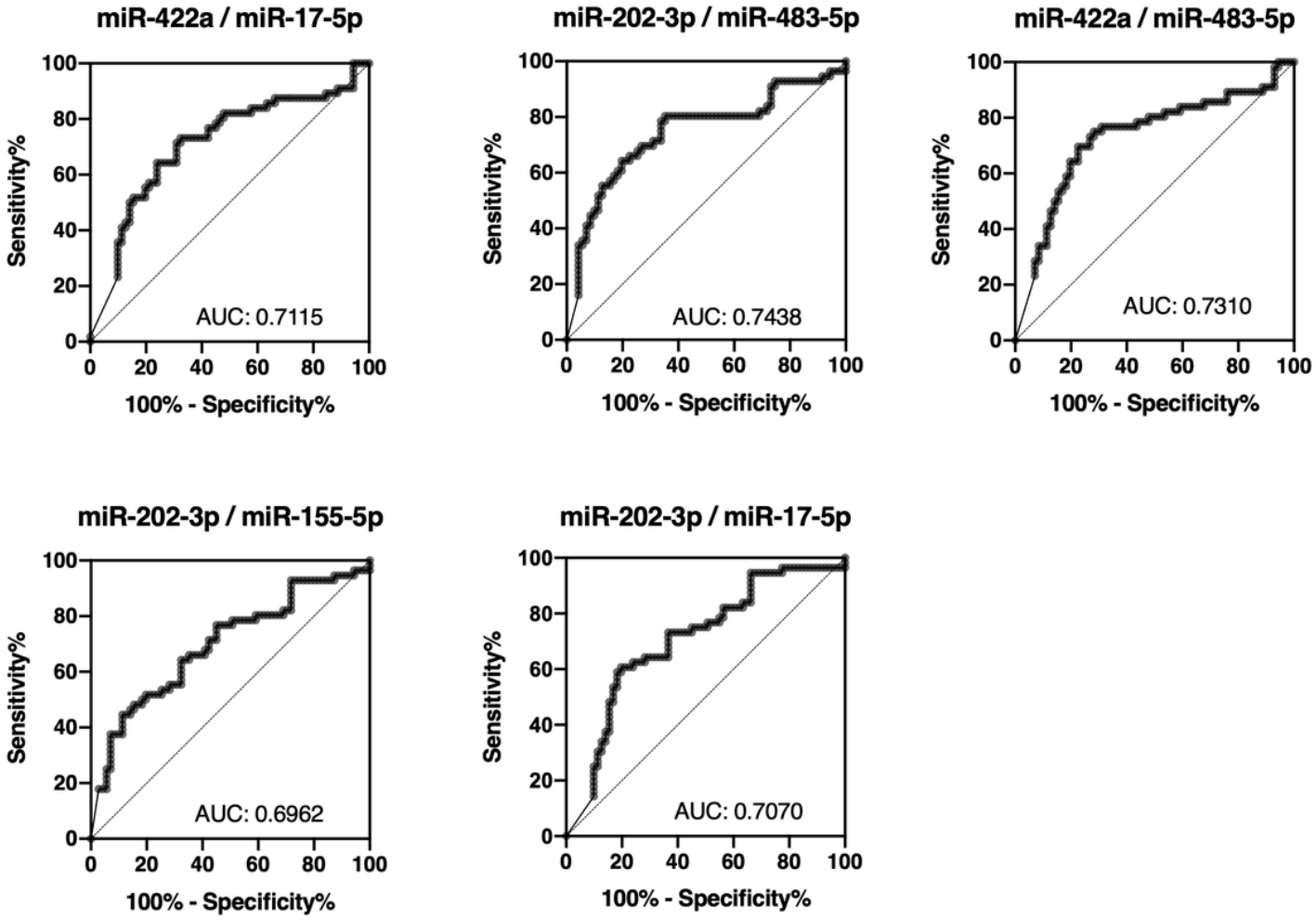

Figure 4

ROC curve of miRNA expression ratios between EPS and non-EPS groups. The top five ratios with higher AUC values including miR-422a/miR-17-5p, miR-202-3p/miR-483-5p, miR-422a/miR-483-5p, miR-202-3p/miR-155-5p, and miR-202-3p/miR-17-5p were selected as candidates for the diagnosis of EPS.

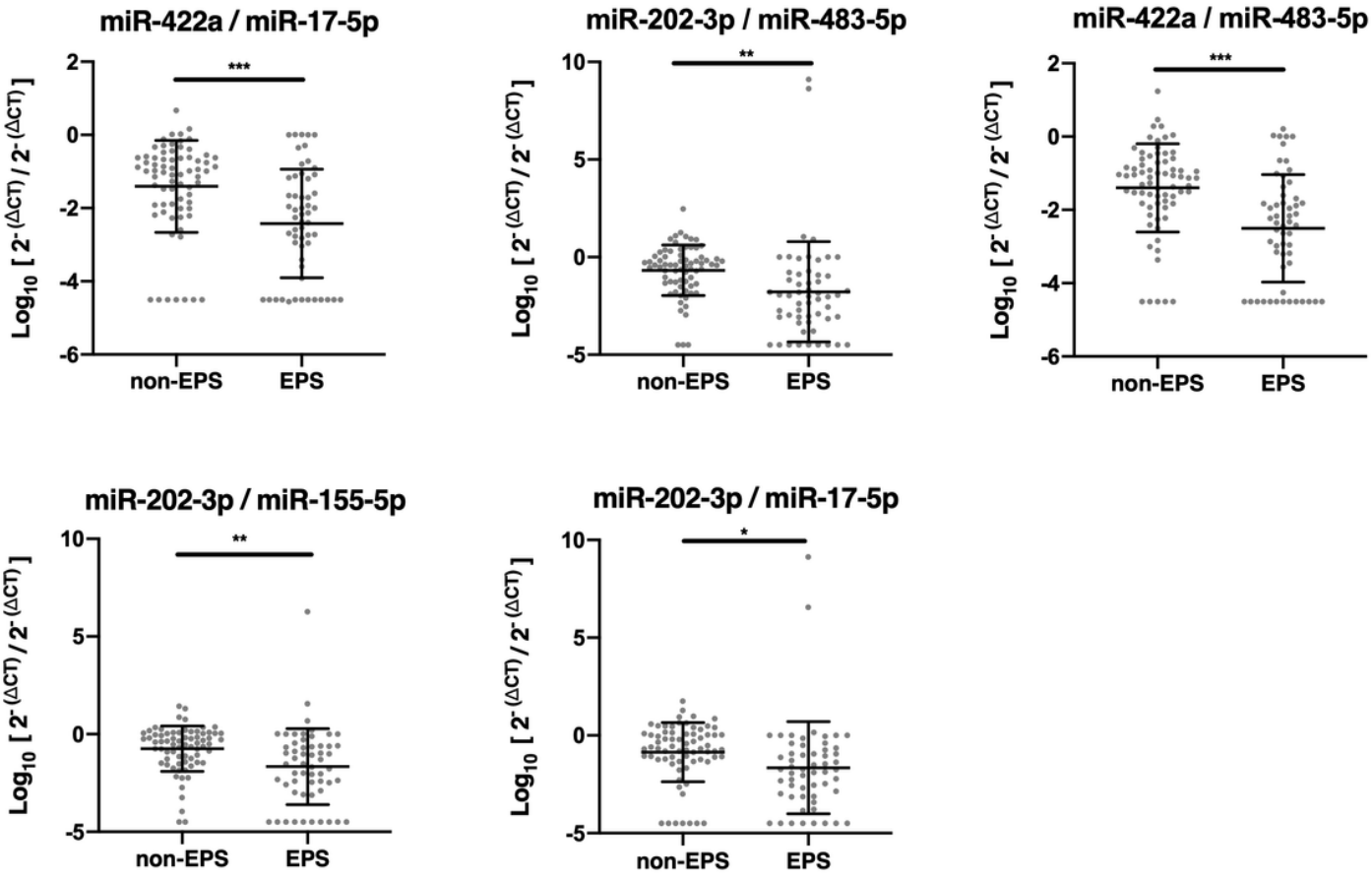

Figure 5

Significant changes in the miRNA expression ratios between the EPS and non-EPS groups. Scatter plots of miR-422a/miR-17-5p, miR-202-3p/miR-483-5p, miR-422a/miR-483-5p, miR-202-3p/miR-155-5p and miR-202-3p/miR-17-5p expression ratios were shown to distinguish between patients with EPS and non-EPS. The Y axis presents the expression level (Log102-ΔCT). The p-value was analyzed by the Student's t-test for each miRNA. *P value < 0.05; **P value < 0.01; ***P value < 0.001

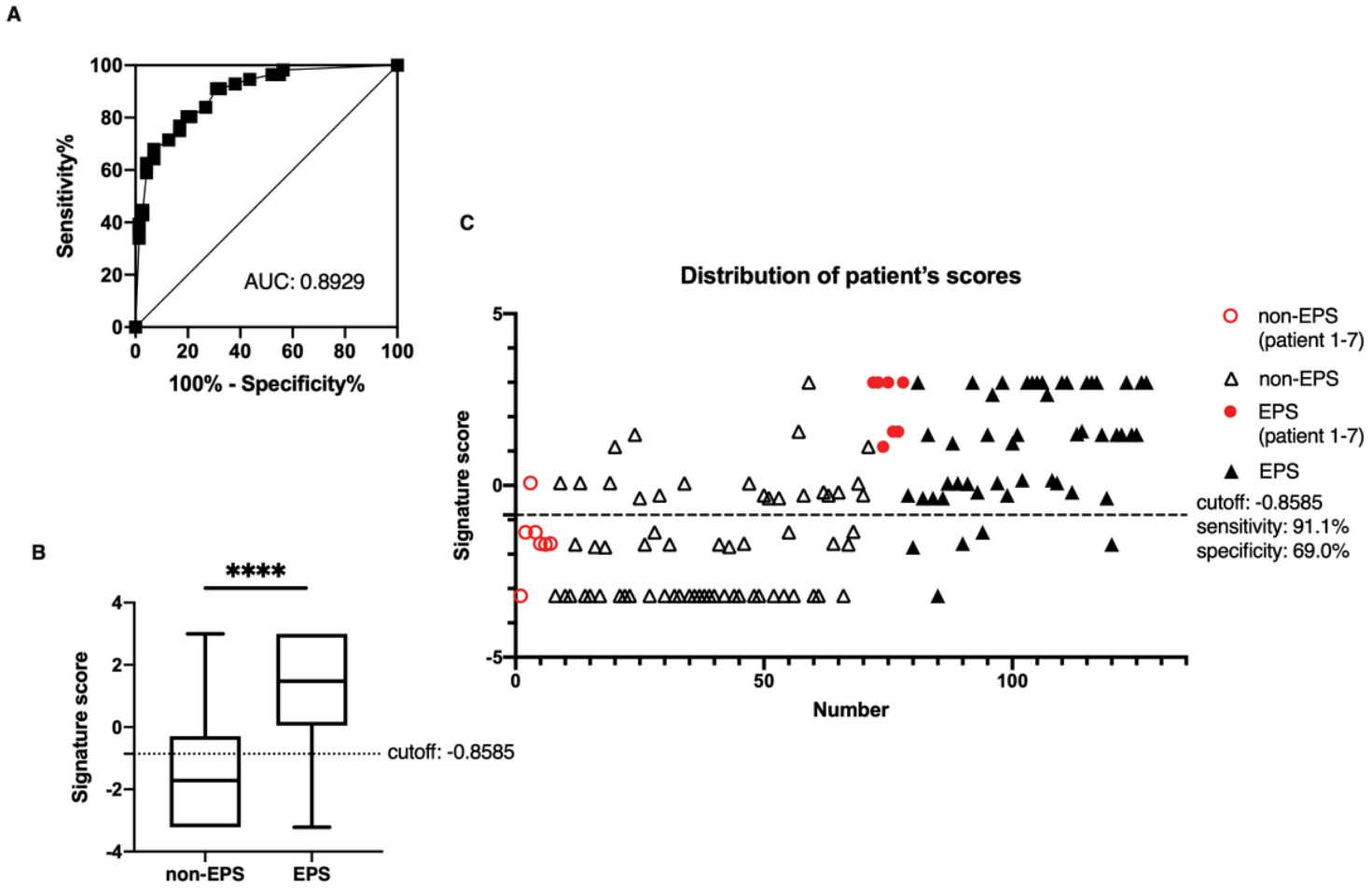

Figure 6

The EPS model of the five miRNA expression ratios. The ROC curve analysis of the five ratios of miR-422a/miR-17-5p, miR-202-3p/miR-483-5p, miR-422a/miR-483-5p, miR-202-3p/miR-155-5p, and miR-202-3p/miR-17-5p was shown to distinguish non-EPS and EPS of PD patients with an AUC of 0.8929 (A). EPS patients had significantly lower signature scores than non-EPS patients (B). The distribution of all patient scores. Using a cutoff value >-0.8585, there was a sensitivity of 91.1% and specificity of 69%. There were differential scores at two time points (red spot, non-EPS and EPS samples from the same PD patient) in seven patients (C). ****P value < 0.001

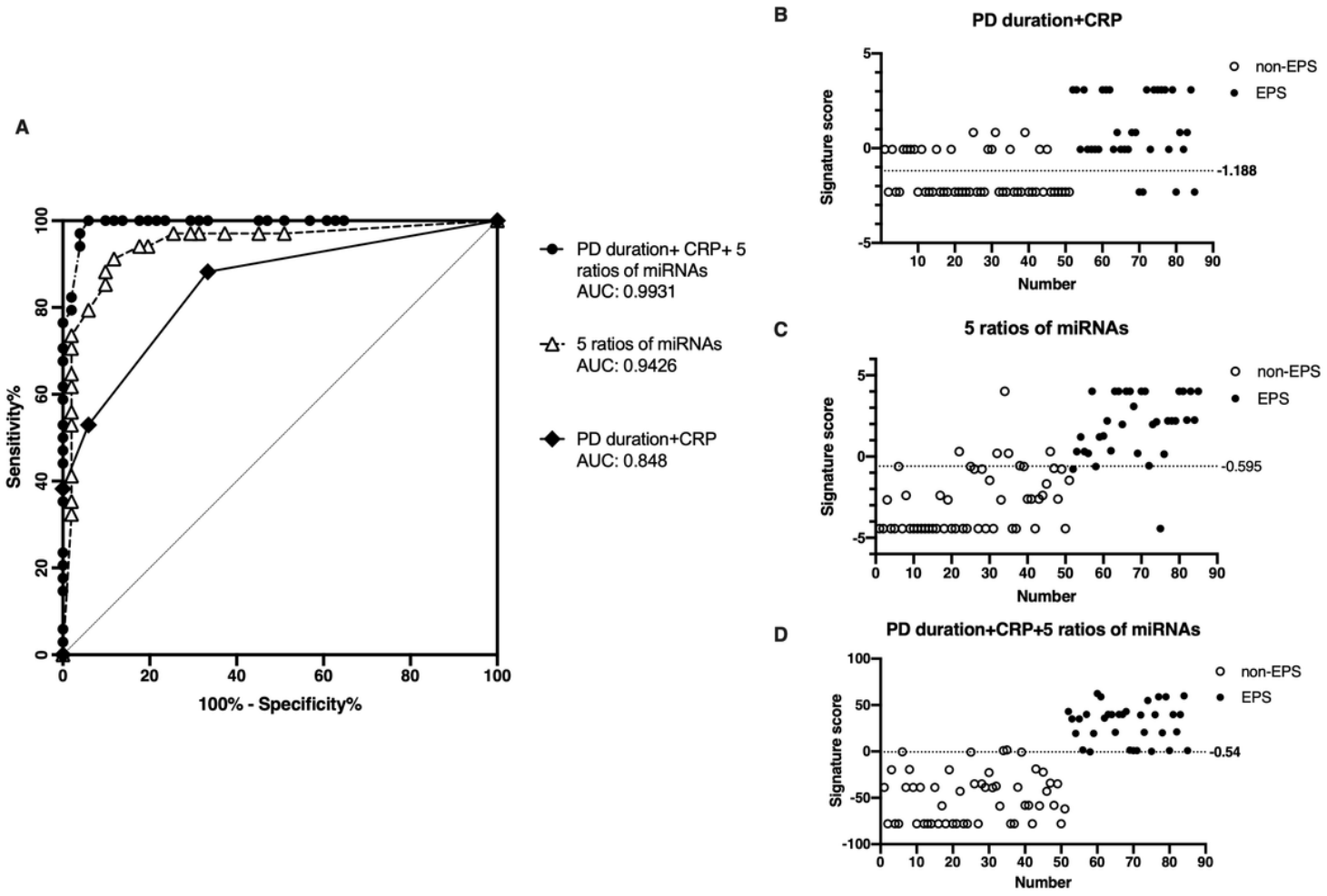

Figure 7

The EPS prediction model with PD duration and CRP level. The ROC curve analysis of two clinical characteristics and the five ratios of miRNA expression was shown to distinguish non-EPS and EPS of PD patients with an AUC of 0.9712 (A). In the score distribution, EPS patients were more accurately estimated with 2 clinical characteristics (PD duration and CRP level) and the 5 ratios of miRNAs (miR-422a/miR-17-5p, miR-202-3p/miR-483-5p, miR-422a/miR-483-5p, miR-202-3p/miR-155-5p, and miR-202-3p/miR-17-5p) (AUC: 0.9931, sensitivity: 100%, specificity: 94.1%) than with 2 clinical characteristics (AUC: 0.848, sensitivity: 88.2%, specificity: 66.7%) or the 5 ratios of miRNAs (AUC: 0.9426, sensitivity: 91.2%, specificity: 88.2%) (B-D).

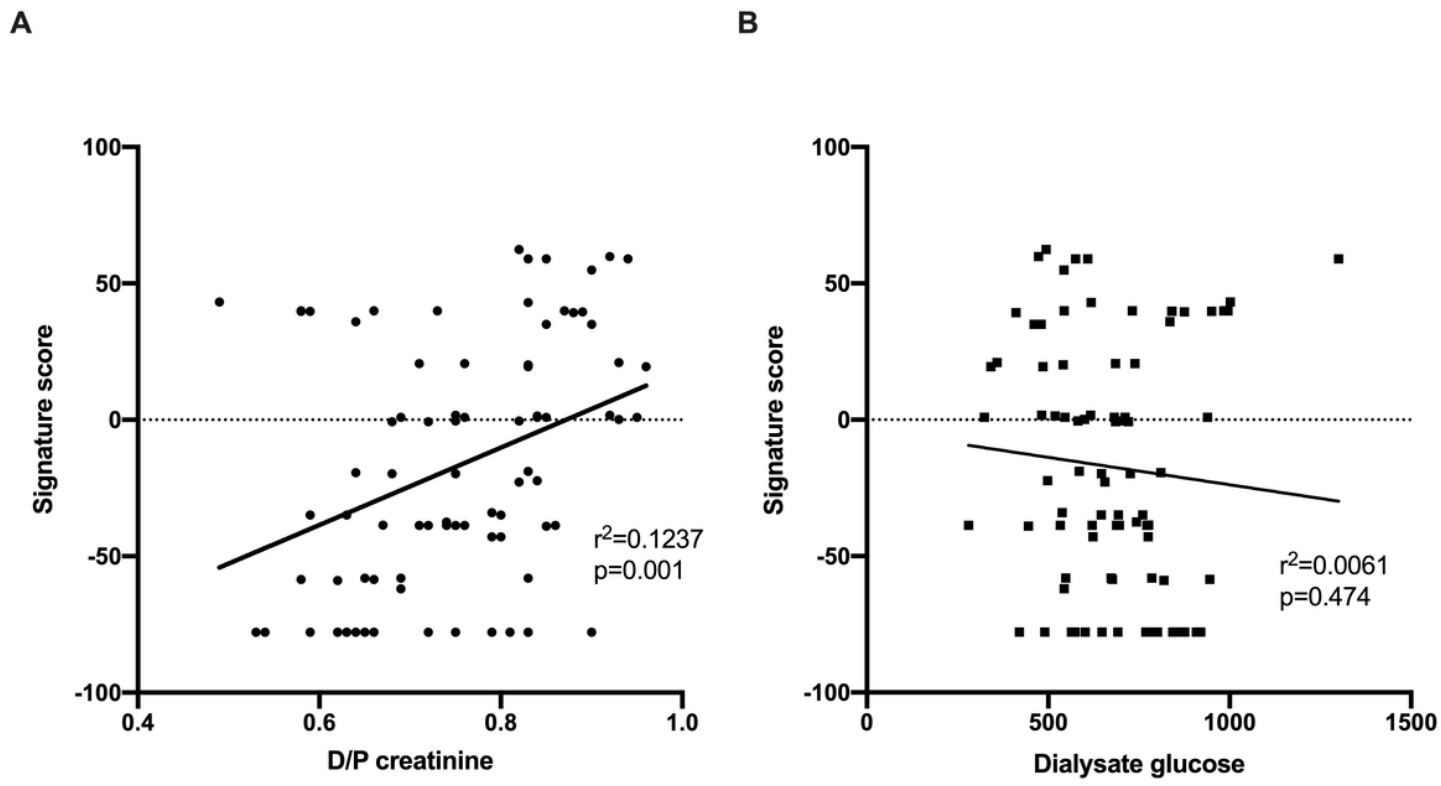

Figure 8

The distribution between the signature score and peritoneal equilibration test with D/P creatinine. The transport rate of creatinine was significantly positively correlated with the signature score from two clinical characteristics and five ratios of miRNA, indicating these scores were linked to the functional impairment of peritoneal membrane. D/P creatinine: the 4-hour dialysate/plasma creatinine.